Extension of the E-Plane Scanning Range in Large Microstrip Arrays by Substrate Modification

Marat Davidovitz, *Member, IEEE*

***Abstract*—The effect of the substrate structure modification on the E-plane scanning performance in large microstrip arrays is studied with the aid of a two-dimensional model. The goal is to alleviate scan blindness effects. The finite-element method of lines is used to solve the electromagnetic equations, thus demonstrating its applicability to open, periodic structures.**

I. Introduction

THE CHARACTERISTICS of infinite phased arrays of microstrip patch antennas have been studied in a number of publications, most notably [1]–[3]. It has been suggested [1], [3] that arrays containing two-dimensional, infinite strip elements represent a useful modeling analogue for patch microstrip arrays, allowing the investigation of the physical phenomena affecting E-plane scan performance parameters with fewer numerical complexities.

In the following communication, improved E-plane scanning performance is reported in two types of arrays with inhomogeneous substrates. In one, the individual strip elements are supported by dielectric slabs of finite extent. In the other, metallic baffles of substrate-height and finite width are used to isolate the array elements.

II. Formulation

Shown in Fig. 1 is a unit-cell in a two-dimensional, infinite and periodic strip array. As in [1], the strip elements are fed by probes, simulated by finite-width current sheets of uniform-density $J_{zp} = 1/(w_p d_{yp})$, where d_{yp} is the probe spacing along the y-direction. The proposed excitation will give rise to three field components, namely $H_y(x,z), E_x(x,z), E_z(x,z)$. The boundary value problem to be solved in each horizontal layer is governed by the following equation

$$\frac{\partial}{\partial x}\left[\frac{1}{\epsilon_r(x)}\frac{\partial H_y}{\partial x}\right] + \frac{1}{\epsilon_r(x)}\frac{\partial^2 H_y}{\partial z^2} + {k_0}^2 H_y = \frac{\partial}{\partial x}\left[\frac{1}{\epsilon_r(x)}J_z\right],$$

where $k_0 = \omega\sqrt{\mu_0\epsilon_0}$, $\epsilon_r(x)$ is the relative *complex* permittivity of the given layer, $J_z = J_{zp}$ in the layer containing the probe; $J_z = 0$, otherwise.

The layer boundaries are defined by the requirement that the dielectric constant be independent of z in each. The conductive portions of the structure, namely the strip and the ground plane, are simulated by using the appropriate conductivity value in the complex permittivity expressions for the corresponding

Manuscript received August 21, 1992.

The author is with the Department of Electrical Engineering, University of Minnesota, Minneapolis, MN 55455.

IEEE Log Number 9204663.

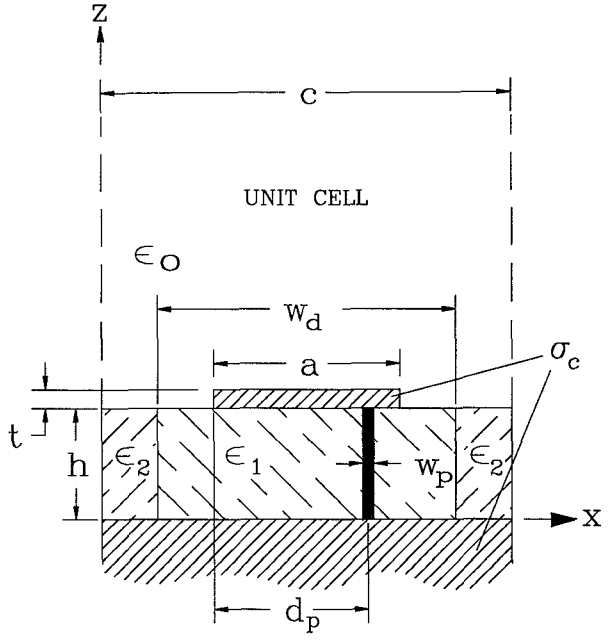

Fig. 1. Unit cell geometry in a strip array.

regions. The electric field components E_x, E_z are derived from H_y via the Maxwell equations. The input impedance is determined by the ratio of the patch-to-ground voltage at the probe and the total input current, with the former represented by the integral of $-E_z(x,z)$ over the probe's length[1].

The magnetic field produced by the infinite phased array is subject to the Floquet boundary condition with a phase shift of $k_x c = k_0 c \sin\theta$ per unit cell, where θ is the scan angle and c the unit cell dimension. To satisfy this condition, H_y is assumed to be of the following form

$$H_y(x,z) = \phi(x,z)e^{-jk_x x},$$

where $\phi(x,z)$ is a periodic function of x, i.e., $\phi(x+c,z) = \phi(x,z)$.

The development of the finite-element method of lines solution is based on a *weak* statement of the problem. It can be shown that an appropriate *weak* formulation of (1) requires $\phi(x,z)$ to satisfy

$$\int_0^c \left\{ -\frac{1}{\epsilon_r(x)}\frac{\partial\phi}{\partial x}\frac{\partial\psi^*}{\partial x} + \frac{jk_x}{\epsilon_r(x)}\left[\phi\frac{\partial\psi^*}{\partial x} - \psi^*\frac{\partial\phi}{\partial x}\right] - \frac{k_x^2}{\epsilon_r(x)}\phi\psi^* + \frac{1}{\epsilon_r(x)}\psi^*\frac{\partial^2\phi}{\partial z^2} + {k_0}^2\phi\psi^* \right\} dx = \int_0^c \left\{ \frac{\partial}{\partial x}\left[\frac{1}{\epsilon_r(x)}J_{zp}\right]\psi^* e^{jk_x x} \right\} dx, \quad (1)$$

TABLE I
ARRAY CHARACTERISTICS

	Fig. 2				Fig. 3		
SFF	1.0	0.9	0.7	0.5	1.0	0.9	0.8
a/λ_0	0.074	0.0725	0.0715	0.075	0.23	0.232	0.218
$Z_b(\Omega)$	35.6	27.4	28.1	38.8	36.2	32.6	30.6
c/λ_0	0.5				0.52		
h/λ_0	0.06				0.1		
ϵ_{r1}	12.8				2.5		
d_p/λ_0	0.9				0.8		
w_p/λ_0	0.005				0.005		
t/λ_0	0.0011				0.0011		
f	10 GHz				10 GHz		
σ_c	$5.8 \times 10^7 \mho - m$				$5.8 \times 10^7 \mho - m$		

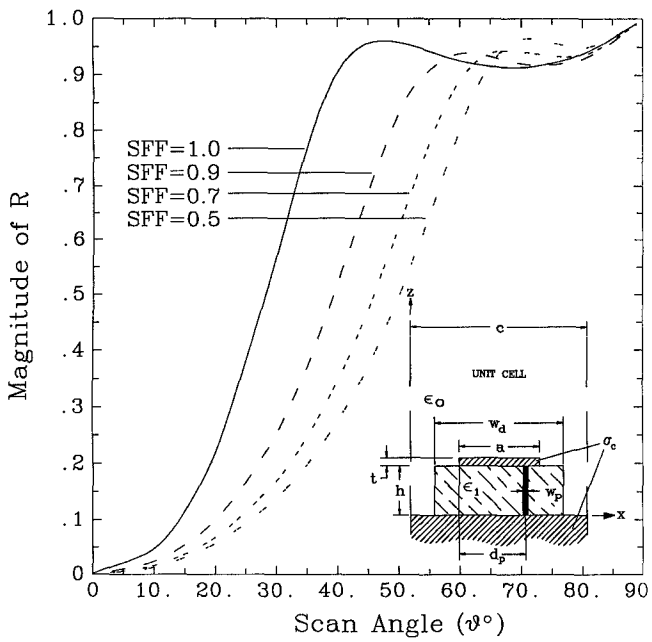

Fig. 2. Scan dependence of the reflection coefficient for a truncated-substrate array.

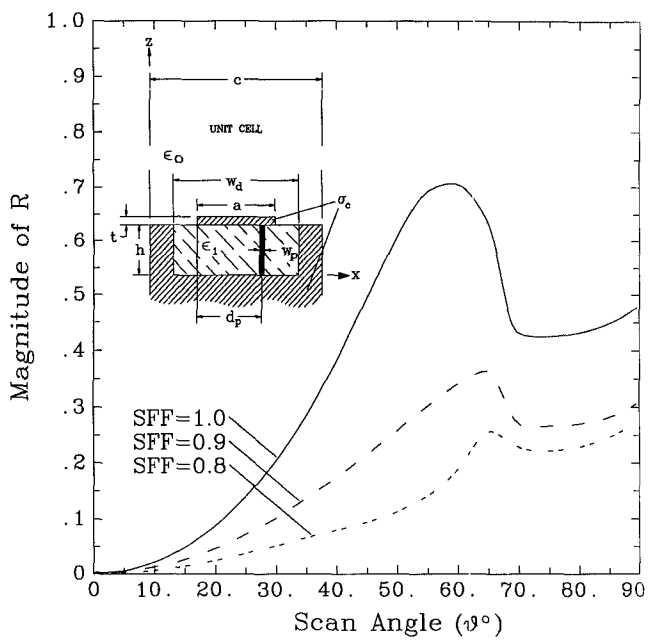

Fig. 3. Scan dependence of the reflection coefficient for a baffle-isolated array.

for *all* values of z and *all* weighting functions $\psi(x)$. The latter, in addition to being periodic (with a period c), must satisfy certain regularity conditions.

The Galerkin finite-element approach is used to discretize (3). The sought solution is expanded in terms of a piecewise linear basis set $\{\Phi_i(x)\}_{i=1}^{N+1}$ as follows

$$\phi(x,z) = \sum_{j=1}^{N+1} v_j(z)\Phi_j(x),$$

where $v_j(z)$ is the value of the approximate solution at the jth finite-element mesh nodal line (x_j, z), and $\Phi_j(x)$ denotes the jth basis function. As required in the Galerkin method, the test functions are drawn from the same basis set.

The outlined procedure yields, after enforcement of the periodic boundary condition, a system of N coupled, ordinary differential equations in the unknowns $v_j(z), j = 1, N$. This differential equation set can be solved analytically, after the unknowns are decoupled by a linear transformation. After obtaining a formal solution for H_y, E_x in each layer, the continuity of these two fields components is imposed (in a weighted average sense) at the horizontal stratification boundaries. The result is a set of complex linear equations which can be inverted to find the unknown coefficients in each layer. The accuracy of the solution was verified by performing relative convergence studies and comparing computed data with those given by Liu *et al.* [1]. The number of basis functions used to compute the results presented in the next section was in the 90–110 range, yielding a final system of linear equations of order 450–550. Solution of this system constituted the primary source of computational expense. Calculation of the input impedance for a single scan angle required approximately 7–10 minutes CPU time on a DEC Station 3100 RISC architecture in the double-precision complex mode. Further algorithm optimization can be expected to significantly reduce the execution time, particularly for greater numbers of horizontal layers.

III. Results and Analysis

The geometrical and material parameters for the arrays considered, as well as the corresponding broadside impedance values Z_b, are summarized in Table I . In all cases the solution was first iterated, with the scan angle set to zero, to determine the resonant strip width. Having thus fixed the patch size, the input impedance was calculated as a function of the scan angle.

In Fig. 2, the effect of substrate (patch support) truncation upon the scan performance is illustrated for an array with $\epsilon_r = 12.8$ substrate. The input reflection coefficient magnitude is plotted as a function of the scan angle for several values of the substrate-fill-fraction (SFF $\equiv w_d/c$), where c is the unit cell size and w_d is the width of the dielectric supporting the patch. The reflection coeficient R was referenced to the input resistance at broadside. In the conventional, contiguous-substrate configuration a blind angle is observed at $\theta \approx 46°$, with $|R| \approx 1$. However, it is clear that even a 10% change in SFF, from SFF $= 1.0$ to SFF $= 0.9$, significantly increases the range over which the input impedance can be matched. Note the apparent movement of the blind angle away from broadside can be attributed to the decreasing reduction in the "average" dielectric constant of the substrate with SFF.

Although substrate truncation appears be effective in modifying the scanning performance of arrays on high-permittivity substrates, it was found to have little effect when the dielectric constant is smaller, e.g., $\epsilon_r = 2.5$. This behavior can be understood in light of the ideas discussed in [1], particularly because in low-permittivity, electrically thiner substrates, the surface wave is loosely bound, becoming leaky when the patch(strip) loading is present. However, data presented in Fig. 3 indicates that notable improvement in scanning performance in this case can be achieved by insertion of thin metallic baffles between the adjacent cells of the array. Although the formulation allows variation of both the height and the width of the inter-cell screens, the former was taken equal to the substrate thickness in order to preserve the dimensional uniformity.

References

[1] C.-C. Liu, J. Shmoys, and A. Hessel, "E-plane performance trade-offs in two-dimensional microstrip-patch element phased arrays," *IEEE Trans. Antennas Propagat.*, vol. AP-30, Nov. 1982.

[2] D. M. Pozar and D. H. Schaubert, "Analysis of an infinite array of rectangular microstrip patches with idealized probe feeds," *IEEE Trans. Antennas Propagat.*, vol. AP-32, Oct. 1984.

[3] J.-P. R. Bayard and D. H. Schaubert, "Finite difference analysis of infinite arrays of two-dimensional microstrip structures," *IEE Proc.*, vol. 137, pt.H, no. 6, Dec. 1990.